

Chapter 3: Hardness

3.1. Introduction

Mechanical strength affects the growth, fabrication and use of non-linear crystals. The hardness can effect how well a crystal can be finished. For instance, the vast majority of high temperature melt grown IR materials typically have low hardness values. This makes it difficult to polish surfaces to high degree of flatness. It also demands that special procedures be implemented to protect the crystal surface from physical damage. Also mechanical strength governs the maximum temperature differential a material can stand before fracture, which is important during growth. While mounting non-linear optical materials for applications involving high laser energies, special considerations must be given to the crystal slip system to prevent a failure of the optical element.

Many materials when subjected to forces or loads can be deformed. Hence it is necessary to know the characteristics of a material such that the resulting deformation will not be excessive and fracture will not occur. Stress is the measure of an applied mechanical load or force, normalised to take into account cross sectional area. Strain represents the amount of deformation induced by a stress. Some of the mechanical properties of the materials can be ascertained by simple stress-strain tests. There are four types of tests: 1) tension, 2) compression, 3) torsion and 4) shear. Tensile test is the most common. Thus depending upon the applied mechanical load or force the material may

experience two kinds of deformation, elastic or plastic. In the case of crystalline solids, the plastic deformation itself is intimately connected to defects, both structural and chemical. Among these defects, the structural defects, viz., dislocations in particular, bear their most pronounced effects on mechanical properties and specifically on hardness. This is so because the plastic flow in a material is determined by density and mobility of dislocations. Although hardness is an empirically defined property, it very efficiently serves the purpose of an over all mechanical characterisation tool and thus can be made to deal with as intrinsic property as the bond strength. It has been rightly termed as a 'strength microprobe'.¹ Deformation in which stress and strain are proportional is called elastic deformation. As the material is deformed beyond this point, the stress is no longer proportional to strain and permanent, non-recoverable, or plastic deformation occurs. Thus the mechanical behaviour of a material reflects the relationship between its response and deformation to an applied load or force. Important mechanical properties are strength, ductility, stiffness and hardness. In this chapter the author discusses to hardness property in general and investigation of the hardness of the ZTS crystals.

The hardness is one of the most important mechanical properties for crystals. The hardness of a material is a poorly defined term, which has many meanings depending upon the experience of the person involved. The scope of hardness properties includes such varied attributes as resistance to abrasives, resistance to plastic deformation, high modulus of elasticity, high yield point, high strength, absence of elastic damping, brittleness, lack of ductility or malleability, high melting temperatures, and magnetic behaviour. Within the scientific community, hardness also represents different concepts. To a metallurgist, it represents resistance to penetration; to a lubrication engineer it

means resistance to wear, whereas it denotes a measure of flow stress to a design engineer, resistance to scratching to a mineralogist, and resistance to cutting to a machinist. Although these actions appear to differ greatly in character, they are all related to the plastic flow stress of the material. In general, hardness usually implies a resistance to deformation, and for crystals/metals the property is a measure of their resistance to permanent or plastic deformation. Hardness tests are performed more frequently than any other mechanical test for several reasons,

- 1) They are simple and inexpensive –ordinarily, no special specimen need be prepared, and the testing apparatus is relatively inexpensive.
- 2) The test is non-destructive- the specimen is neither fractured nor excessively deformed; a small indentation is the only deformation
- 3) Other mechanical properties often may be estimated from hardness data, such as tensile strength.

Particular emphasis is placed on those applications in which the hardness test, as a means of applying concentrated or point loads, has been used to advantage in studies on a) Occurrence of Plastic deformation, b) identification of slip systems and twinning planes, and c) dynamic behaviour of dislocations in crystals.

Earlier methods of testing hardness generally consisted of scratching. One of the earliest forms of scratch testing goes back to Reaumur in 1722.² In 1822, the Mohs scale of hardness was introduced for minerals and measures the relative hardness of ten minerals. In the late 19th century, more attention was paid to hardness and its measurements. Brinell, a Swedish engineer, presented a paper to the Swedish Society of Technologists describing his “ball’ test. This rapidly became known as the Brinell test

and became universally used in the metal working industry. Because of the limitations imposed by the Brinell method and increased engineering requirements, several investigators intensified their efforts towards, devising other indenters. There are three general types of hardness measurements depending on the manner in which the test is conducted. These are:

- 1) scratch hardness
- 2) static or indentation hardness and
- 3) rebound, or dynamic hardness.

Scratch hardness is of primary interest to mineralogist. With this measure of hardness, various minerals and other materials are rated on their ability to scratch one another. A different type of scratch-harness test measures the depth or width of a scratch made by drawing a diamond stylus across the surface under definite load.³ In dynamic-hardness measurements the indenter is usually dropped onto the metal surface, and the hardness is expressed as the energy of impact. The indentation-hardness is of major importance to engineers and for researchers in the field of characterisation of crystals and in trying to study the various properties of crystals. In its simplest and most popular form, the static-indentation test, an indenter of specific geometry is pressed into the surface of a test specimen under a known load.

Upon the removal of the indenter, a permanent impression is retained in the specimen. The mean pressure or hardness is defined as a load divided by area of the impression. By suitable choice of indenter material and relatively simple equipment construction, this type of hardness test (as well as others) can be easily applied to all

crystalline materials under various conditions of temperature and environment. The various types of indentation hardness namely,

- 1) Brinell Hardness.
- 2) Meyer Hardness
- 3) Rockwell Hardness
- 4) Vickers hardness

The requirement of hardness determination over very small areas led to development of the “microhardness testers”. The use of the scratch-hardness test for these purposes was mentioned earlier but an indentation-hardness test was found to more useful.⁴ These led to the development of various microhardness testers like

- 1) Knoop indentation microhardness tester
- 2) Tukon microhardness tester
- 3) Eberbach microhardness tester
- 4) Bergsman’s microhardness tester
- 5) Vickers microhardness tester.

The term “microhardness” usually refers to indentation hardness tests made with the loads that do not exceed 1-Kg. Such tests have been made with a load as light as 1 g, although the majority of microhardness tests are made with loads of 100 to 500g. In general, the term is related to the size of the indentation rather than to the load applied. Development of the Knoop test by the National Bureau of standards in 1939 and the Vickers test (also called the diamond pyramid hardness test) in England in 1925 has made microhardness testing a routine procedure. Both of these tests use precisely shaped diamond indenter and various loads to determine hardness of a wide variety of materials.

Microhardness testing is capable providing information on the hardness characteristics of materials that cannot be obtained with hardness tests such as the Brinell and Rockwell. Because of the required degree of precision for both equipment and operation, microhardness testing is usually, although not necessarily, performed in a laboratory. Microhardness testing is recognised as a valuable method for controlling numerous production operations in addition to its use in research applications. Specific fields of applications of microhardness testing include:

- Measuring the hardness of precision workpieces that are too small to be measured by the more common hardness testing methods.
- Measuring the hardness of product forms like foil or wires are too thin or too small in diameter to be measured by the more conventional methods.
- Monitoring carburizing or nitriding operations, which is usually accomplished by hardness surveys taken on cross sections of test pieces that accompany workpieces through production operations.
- Measuring the hardness of individual microconstituents.
- Measuring hardness close to the edges of workpieces, thus detecting undesirable surface conditions such as grinding burn and decarburization.
- Measuring the hardness of surface layers such as plating or bonded layers.

In such case the microhardness testing is done with one of the two diamond pyramid indenter, the Vickers (also referred to as Diamond Pyramid) or the Knoop. The Vickers indenter used for microhardness testing is the same geometric form as is used for conventional Vickers testing. The depth of the Vickers indentation is approximately one seventh of the diagonal. The choice between the Knoop and Vickers indenters is

sometime arbitrary. Because the Vickers indenter penetrates deeper into the specimen than the Knoop indenter, the Vickers is less sensitive to surface conditions. However, because the Vickers indenter has shorter diagonals, it is more sensitive to measurement errors compared to the Knoop indenter. The hardness value for either Vickers or Knoop is a stress value and is expressed as Kilograms per square millimetre or Megapascals (Mpa). Nowadays automated set-ups for microhardness testing are also available. Indentations are made automatically at pre-established locations on the work piece. Since in the present investigation the Vickers Diamond Pyramidal indenter has been used, the indenter and its application will be described in detail.

3.2. Vickers Hardness Tester

3.2.1. Principle of Vickers Hardness Tester:

The 136° diamond pyramid hardness tester, commonly referred to as the Vickers tester, was introduced in England in 1925 by R. Smith and G. Sandland.⁵ Its early acceptance by industry was limited to the largest laboratories, and its use was chiefly for research purposes.

Figure 3.1 shows the Vickers indenter. The diamond pyramid hardness method follows the Brinell principle in that an indenter of definite shape is pressed into the material to be tested, the load removed, the diagonals of the resulting impression measured, and the hardness number calculated by dividing the load by the surface area of indentation.

The indenter is made of diamond, and is in the form of a square-base pyramid having an angle of 136° between faces. This indenter thus has angle across corners, or so-called

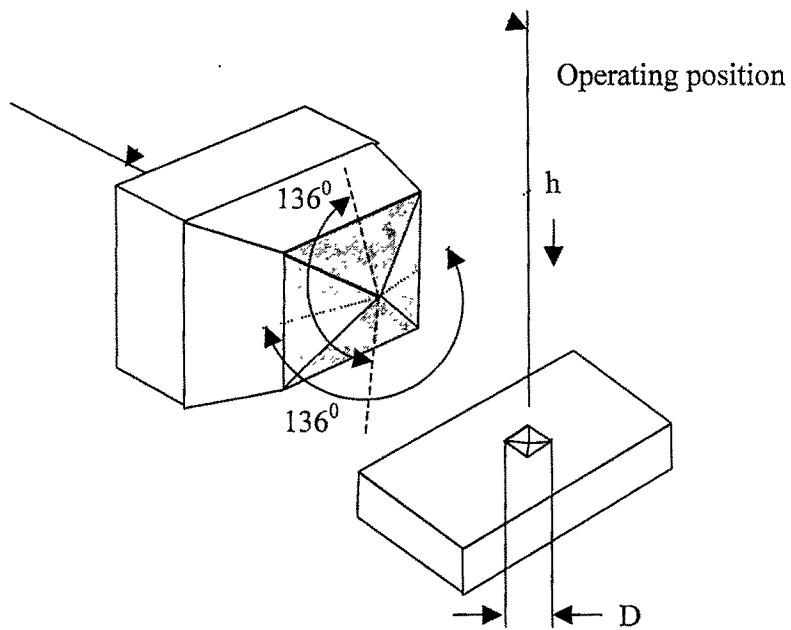


Fig. 3.1. Diamond pyramid indenter used for Vickers hardness testing and resulting indentation in the workpiece. D is the mean diagonal of indentation. (Metals Handbook, Mechanical Testing, Vol. 8, 9th ed., ASM, 1985, p. 91)

edge angle, of $148^{\circ} 6' 42.5''$. The facets are sharply polished, free from surface imperfections and the point is sharp. The diamond pyramid hardness number, often designated as DPH, is the quotient of the applied load divide by the pyramid and surface area of the impression and is obtained as:

$$DPH = 9.8 \times \frac{1854 \cdot P}{d^2} \text{ MPa ,}$$

where P = load in gms (for microhardness)

d = diagonal in μm

θ = Angle between opposite faces of the diamond = 136°

The factors that affect the indentation process by a microhardness tester are:

- The optical equipment used in microhardness testers
- Mechanical vibrations, if any, during the indentation process
- Surface finish of the specimen
- Accuracy in determining the load P and in measurement of the indentation diagonal d .

3.3. Hardness Number vs Load:

Prior to the advent of the microhardness tester, it was assumed that the Vickers indenter (as well as other indenters giving geometrically similar indentations) produced a hardness number that was independent of the indenting load. This generally can be accepted for loads of approximately more than 100 g since; in the low load range the Hardness becomes a function of the magnitude of the test load. When using very light loads, some observers have noticed an increase in microhardness values with increasing

load. This is followed by a range in which the hardness becomes independent of the load and approaches a constant value identified as the '*Vickers Curve*'. This effect occurs with a wide range of materials, from those as soft as copper to fully hardened steel. Before these studies were made, most engineers felt that the Vickers hardness and the Knoop hardness, because of geometrically similar indentations, should be independent of the load.

The apparent increase in hardness with decrease in load (in properly prepared surfaces) is primarily caused by

- 1) Errors in the determination of the size of the indentation and
- 2) Aberrations in the elastic recovery of the indentation.
- 3) Strain hardening phenomenon dominant for small penetration depths into surface layers.

As the size of the indentation decreases, the measurements will have less relative accuracy due to various factors like the complexity of the stress-strain curve of the material at such range of loads, microstructural defects like impurities in surface layers, etc.

Other explanations of load dependence may be found in the design of the microhardness tester or in the testing procedure. Shape of the indenter, vibrations, microscope, friction of the test surface with the tester, surface preparation and cold working, in addition to size of the indentation, elastic recovery, formation of a bulge or other characteristics of the indentation itself, can affect the microhardness readings in varying ways, depending on the load.

In microhardness tests, it would seem likely that the load dependence is based to some extent on elastic recovery of the indentation after the load is removed. However, experimental studies have indicated that elastic recovery of Vickers indentation is too small to explain load dependence completely. Another factor that must be considered is that the square of the Vickers indentation often deviates from the square form. This is caused by the formation of a bulge at the sides of the indentation.

From a practical standpoint, however, load dependence is not as important as some may believe. The choice of load depends on the size and depth of indentation considered to be most desirable. Generally, the indentation is made as large as practicable to obtain the greatest accuracy possible and thus obtaining the true hardness of the bulk of the specimen since surface effects become insignificant at large penetration depths. As long as a single load is used through a series of tests, the load dependence is of little significance. In principle, using different loads in any particular investigation alters the as-measured hardness numbers; the lighter the load, the more significant the change.

3.3.1. Vickers Hardness versus Load studies in ZTS crystal

There are few reports on the μ measurements of hardness anisotropy (discussed later in the chapter) on the ZTS crystal, however, no reports were found on the Vickers hardness measurements on this crystal. The author has carried out the Vickers hardness studies on the three major planes of this crystal. For the Vickers hardness tests and measurements, the Vickers pyramidal diamond indenter and the microhardness accessory on the Vickers Projection Microscope were used.

The Vickers microhardness indentations were produced on the individual planes, (001), (010) and (100) under the applied loads in the range of 49-980 mN with constant azimuthal orientation of the indenter and a constant loading time of 15s at room temperature. The reference 0° orientations of the indentation mark diagonals along the three planes, (100), (010) and (001), were chosen to be [010], [001] and [010], respectively. The measurement of the indentation diagonal length was made to an accuracy of $0.190 \mu\text{m}$ (using a micrometer eyepiece precalibrated against the standard graticule supplied with the hardness tester), and that of the load was to an accuracy of 2.5 mN. Precautions were taken to avoid any kind of vibrations during the measurements.

The variation of H_v with load P was obtained as shown in figure 3.2. Figure 3.2 clearly shows the complex load dependence of hardness. At low loads, the hardness increases with increasing load and exhibits a peak before reaching saturation at higher loads. Similar load dependence of hardness at low applied loads has been observed in a number of cases, particularly the case of a TGS crystal, which is also a ferroelectric crystal.^{6,7} This behaviour has been explained in terms of hardening of surface layers by progressive penetration of the indenter and the finite penetration depth to reach saturation termed as the deformation-induced coherent region. The saturation hardness is then known to represent the true bulk material hardness. Thus it is observed that (100) is the hardest of the three planes: $H_v(100) \sim 8240 \text{ Mpa}$, $H_v(010) \sim 1727 \text{ Mpa}$, and $H_v(001) \sim 981 \text{ Mpa}$.

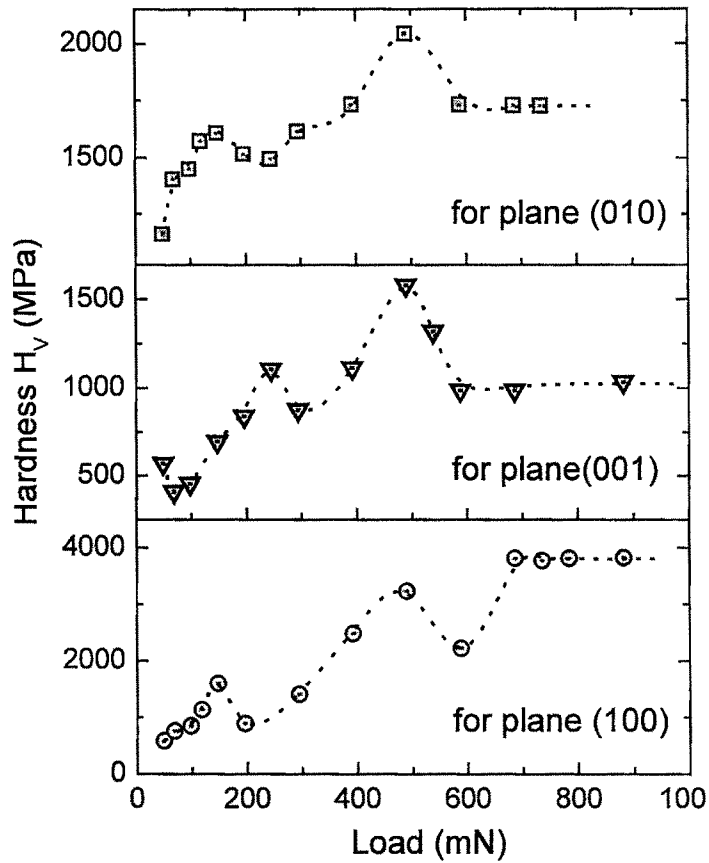


Fig. 3.2. The applied load dependence of Vickers hardness, H_v , of (010), (001) and (100) planes. The hardness curves level at larger loads. This value is reported as the bulk hardness of the crystal.

3.4. Hardness Anisotropy

Many solids especially crystals are plastically anisotropic, i.e., their hardness in one direction is different from that in the other direction and the hardness values measured on different planes are also different. This is true even for cubic crystals because the critical shear stress for plastic flow is dependent on the plane of observation. In principle, any kind of hardness test can be used to characterise the variations in the strength of materials in three principal directions of anisotropy. They could be the diamond pyramid indenter or even the spherical indenters, so long as the indentation load is sensitive enough to respond to the differences in the strengths of materials. If however, the material has planar anisotropy, that is, the strength varies along different directions in a given plane, the spherical indenters cannot be used to distinguish such variations.

Such directional effects have been reviewed by Brookes *et al*⁸ and are most effectively obtained using a Knoop indenter giving its impression on the working surface with the ratio of diagonals 7:1. However, Vickers pyramidal indenter and Berkovitch triangular indenter also show similar variations in hardness. In the present study of hardness anisotropy, the hardness is measured for various azimuthal orientations of the indenter loaded perpendicular to the crystal surface under study.

It is well known that the nature of hardness anisotropy in crystals is determined by the crystal structure of the material and the primary slip systems that accommodate dislocations motion during indentation. In the last decade Rowcliffe and Hollox⁹ and Hannik *et al.*¹⁰ have made extensive studies to establish the active slip systems and the

conditions governing choice of slip systems by using the analysis of hardness anisotropy. Thus in order to understand the hardness anisotropy in a crystal and to correlate the orientation dependence of indentation hardness of crystalline solids with plastic deformation, concept of an “Effective Resolved Shear Stress (ERSS)” on a slip system has been very useful. In 1949 pioneering analysis of Daniels and Dunn sought to explain the orientation dependence of the Knoop hardness for silicon iron crystals and for zinc crystals on the basis that the state of stress for an indentation could be approximated by a constrained tensile test and that the hardness was determined by an effective resolved shear stress, directly analogous to the critical resolved shear stress which is required for the onset of plastic flow.¹¹ However their theory had several deficiencies. This analysis was then re-examined and modified. The ERSS for a particular slip system is generally calculated using the equation by Brookes *et al.*, which is discussed further in this chapter.¹²

3.4.1. Vickers Hardness Anisotropy in ZTS crystal

For the Vickers hardness anisotropy studies, indentations were produced on the individual planes (100), (010) and (001), at different orientations at the intervals of 10° under a constant applied load of 200 mN and a constant loading time of 15 seconds. The reference 0° orientations of the indentation mark diagonals along the three planes, (100), (010) and (001), were chosen to be [010], [001] and [010], respectively.

From figure. 3.3 it can be seen that the variation of the hardness, H_v , obtained on the three planes has been found to repeat for every 90° interval indicating the four-fold symmetry of the indenter superposed on the two-fold symmetries present in the crystal.

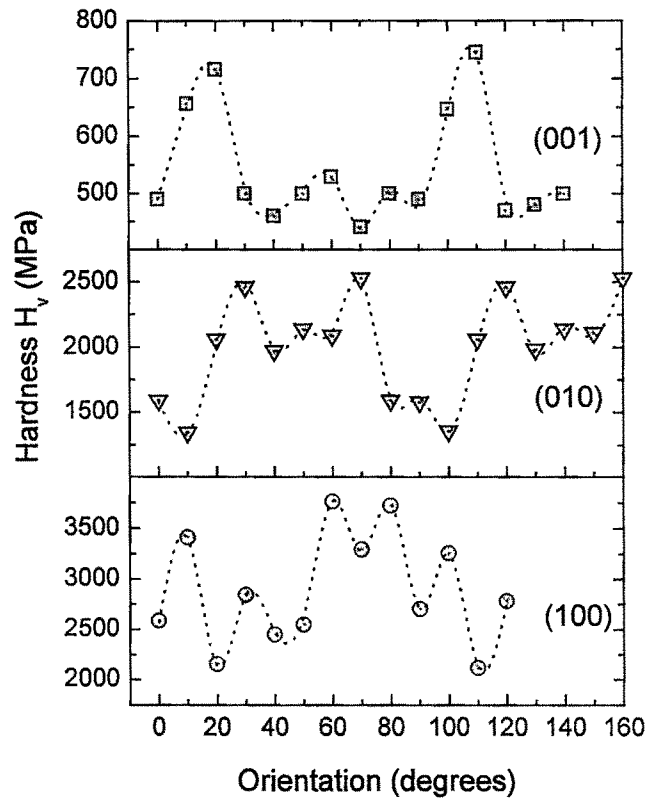


Fig. 3.3. Hardness versus crystal orientation for (001), (010) and (100) planes.

The hardest and the softest directions on the three planes were analysed stereographically giving the results shown in Table.4.1.¹³

Table. 3.1

Plane	Hardest Directions	Softest Directions
(100)	[012]	[011]
(010)	[10 $\bar{2}$]	[10 $\bar{3}$]
(001)	[2 $\bar{1}$ 0]	[210]

The surface-anisotropy variations in the hardness of (100), (010) and (001) are observed to be to the extent of 35%, 49% and 32%, respectively. The hardness anisotropy coefficients of the planes (100), (010) and (001), i.e. the ratios of the difference of the maximum and minimum hardness values to the maximum value, are found to be 0.35, 0.49 and 0.42, respectively. The hardness anisotropy so far reported for this crystal has been in terms of the Knoop hardness of (100).¹⁴ However, no assignment of the hard/soft direction is available for comparing with our results. The author, in the following chapter, has discussed the relation between the hard/soft direction and the laser damage results.

3.4.2. Surface Anisotropy of Hardness and Effective Resolved Shear Stress on the slip system of ZTS crystal:

It is known that the slip mechanism is responsible for accommodating the largest part of plastic deformation of crystals. The slip usually takes place along preferred planes and directions and the amount of deformation would therefore depend on the orientation of the deforming stress axis relative to the slip plane and slip direction in the crystal in addition to the magnitude of the applied load. The minimum shear stress resolved along the slip direction to cause the slip deformation is known as the Critical Resolved Shear Stress (CRSS). Hence the larger the Effective Resolved Shear Stress (ERSS), the larger will be the deformation and the smaller will be the hardness. This obviously implies that the hardness anisotropy can be explained in terms of anisotropy in the ERSS on the active slip system of the crystal. This fact has been used to interpret the results of hardness anisotropy obtained on two of the major habit planes of the ZTS crystal, viz., (100) and (001). The slip system of the crystal, viz., (012) [100], has been assumed on the basis of the dislocation etching studies discussed in Chapter 2. The calculation of the ERSS values was done by using the following relation by Brooks *et al.*¹²

$$ERSS = \frac{F}{2A} \cdot \cos \phi \cdot \cos \lambda \cdot (\cos \psi + \sin \gamma)$$

where F = applied force, A = area supporting F , ϕ = angle between axis of F (normal to the indenter face) and the normal to the slip plane, λ = angle between axis of F and the slip direction, ψ = angle between the axis, H , normal to F and lying in the indented

surface (this amounts to the intersection edge of the indenter face with the indented surface) and the axis of rotation, AR , of the slip system (axis normal to the slip direction and lying in the slip plane) and γ = angle between H and the slip direction. Taking the factor $F/2A$ as an undetermined constant, the above relation is used to obtain relative values of ERSS. As mentioned earlier, to study the surface anisotropy of hardness, the hardness is measured for various azimuthal orientations of the indenter, hence the angles ϕ , λ , ψ and γ with the rotation of the indenter about its loading axis with respect to a reference direction in the surface. It is also obvious that the variations of the angles, in general, is not of a universal nature but depends in a complicated way on the relative dispositions of the slip elements around the rotation axis of the indenter and hence will differ from crystal to crystal and from surface to surface of a given crystal. The angles discussed in the above equation are shown schematically on the (100) and (001) stereographic projection in figure 3.4 and 3.5 respectively, for the initial azimuthal orientations of the indenter corresponding to the respective crystal planes. These orientations correspond to the indentation diagonal set parallel to the direction [010] belonging to both the planes. The stress axis being normal to the indenter surface subtends an angle of 22° with the loading axis (normal to the crystal surface) and is shown (for one of the indenter faces) as F . SD , SP , AR , H and ID in the diagrams indicate projections of the slip direction, the slip plane normal, the axis of rotation of the slip plane, the edge of the indenter and the indentation diagonal, respectively. **The angles in the Brooke's formula thus get defined in the present case as :**

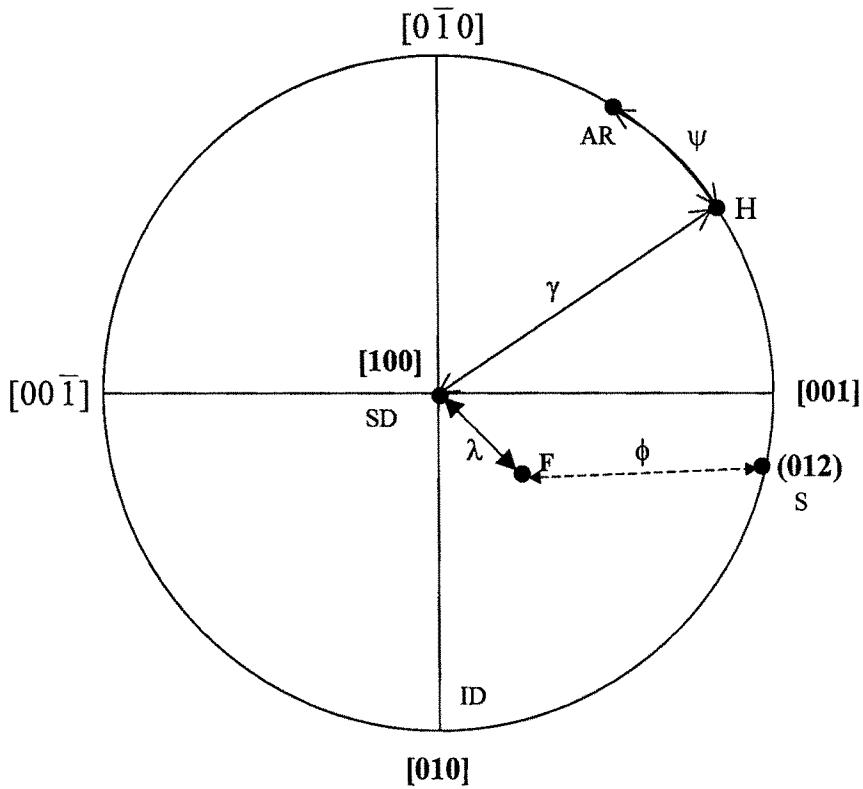


Fig. 3.4. Stereographic projections of the slip and the indenter elements on the (100) plane and the angles in the ERSS formula. .

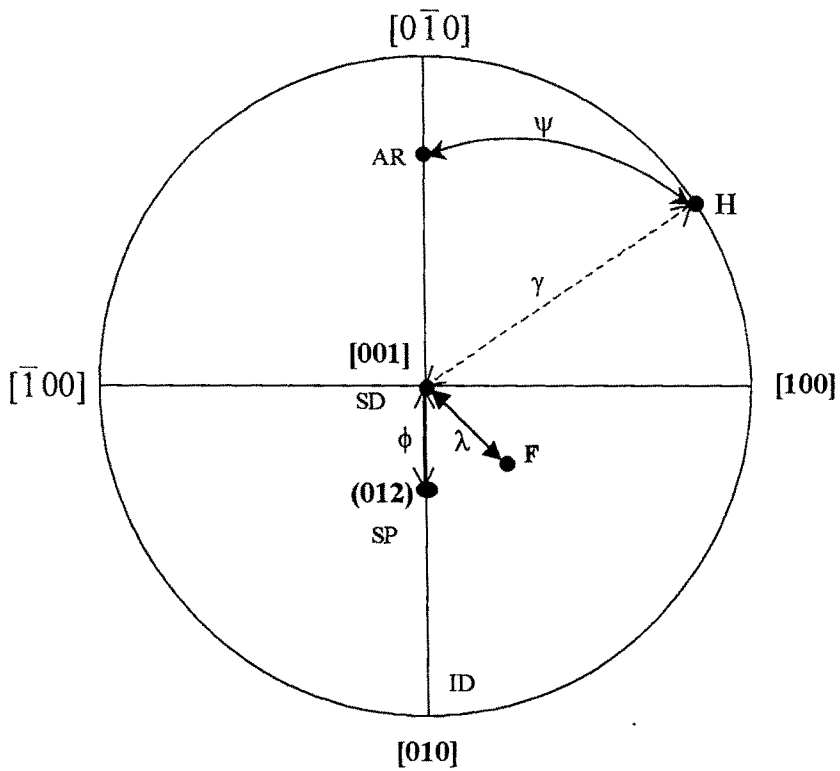


Fig. 3.5. Stereographic projections of the slip and the indenter elements on the (001) plane and the angles in the ERSS formula.

ϕ = angle between F and SP , i.e. F and (012)

λ = angle between F and SD , i.e. F and $[100]$

Ψ = angle between H and AR , i.e. H and $[01\bar{2}]$ or $[0\bar{1}2]$

γ = angle between H and SD , i.e. H and $[100]$

V. P. Bhatt *et al*¹⁵ have given a formula to evaluate these angles in various azimuthal orientations of the indenter:

$$\rho' = \cos^{-1} \{ \sin \rho \cos [\chi_o + \beta + (\eta - 1)90^\circ] \sin \theta + \cos \rho \cos \theta \}$$

where ρ' would be the angle to be calculated, i.e., ϕ, λ, Ψ or γ in the ERSS relation described above. Here,

χ_o = starting angle between the projection of the appropriate slip element (SP, SD or AR as the case may be) and the projection of the appropriate indenter element (F or H as the case may be)

θ = angle between slip element and indented plane normal,

β = azimuthal orientation angle,

η = facet number of the indenter, ($\eta = 1, 2, 3$ and 4) and

ρ = angle between projection centre and F (or H).

$\rho = 22^\circ$ (or 90°)

Thus the angles ϕ, λ, Ψ and γ angles were calculated for indentations at various azimuthal orientations in steps of 10° on the planes (100) and (001) .

For the (100) plane of indentation and [010] as the reference direction,

ρ' will be,

ϕ , when, χ_o = angle between the projection of slip plane (012) on (100) plane and F
= 42° .

λ , when, χ_o = angle between the projection of slip direction [100] on (100) plane and F
= 90°

ψ , when, χ_o = angle between the projection of axis of rotation AR on (100) plane and H
= 76° .

γ , when, χ_o = angle between the projection of slip direction [100] on (100) plane and H
= 90° .

As explained earlier that θ = angle between slip element (SP , SD and AR) and the centre of projection (i.e. working plane), and so

θ = 90° when calculating ϕ .

= 0° when calculating λ .

= 90° when calculating ψ .

= 0° when calculating γ .

Using these values, the ERSS was calculated for various azimuthal orientations of the indenter from 0° to 120° in steps of 10° relative to the reference direction in the surface.

The mean of these values over the four faces of the indenter for each orientation was

calculated. The mean ERSS thus obtained is plotted against the azimuthal orientation (Figure 3.6).

Similar calculations were done for the indentations on (001) plane, using the starting configurations of slip and indenter elements shown in the Figure 3.5 and the values of ϕ , λ , Ψ or γ are obtained. Using these values, the ERSS was calculated for various azimuthal orientations of the indenter and plotted against azimuthal orientation, Figure. 3.7

The plots of H_v versus orientation θ obtained for the planes (100) and (001) are also shown in Fig. 3.6 and Fig. 3.7. Since the deformation would be more when the resolved shear stress on the slip system is more, the smaller the ERSS the greater should be the hardness and vice-versa. Ideally thus, the ERSS and H_v should bear an inverse relation. The plots obtained satisfy this to a good extent, although the relative increase or decrease in one quantity may not exactly be reflected in the relative increase or decrease in the other quantity. Within an approximation, the anisotropy results also confirm the slip system to be (012) [100], responsible for the plastic deformation of the crystal.

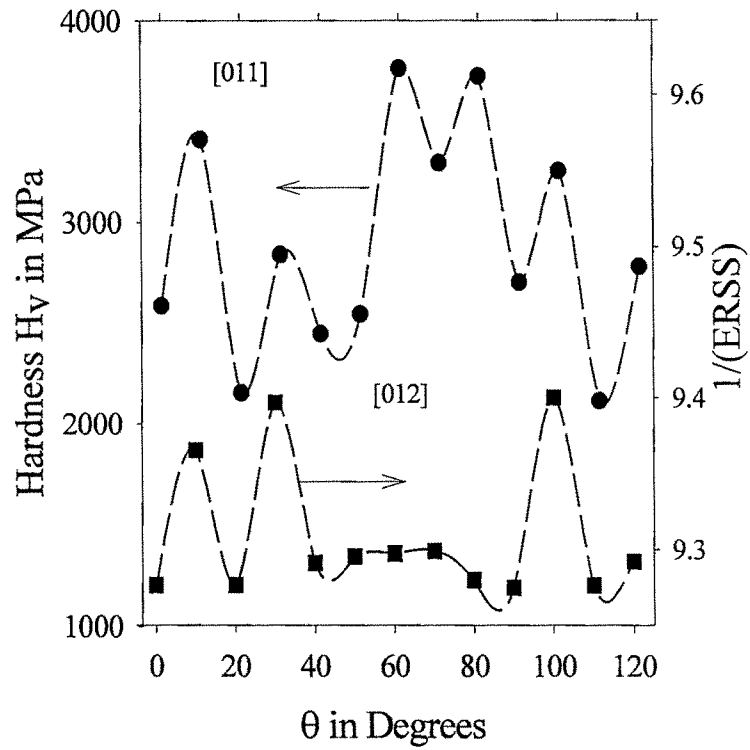


Fig. 3.6. Plots of Hardness, H_V , of the (100) plane and the reciprocal of the effective resolved shear stress versus azimuthal orientation of the indenter.

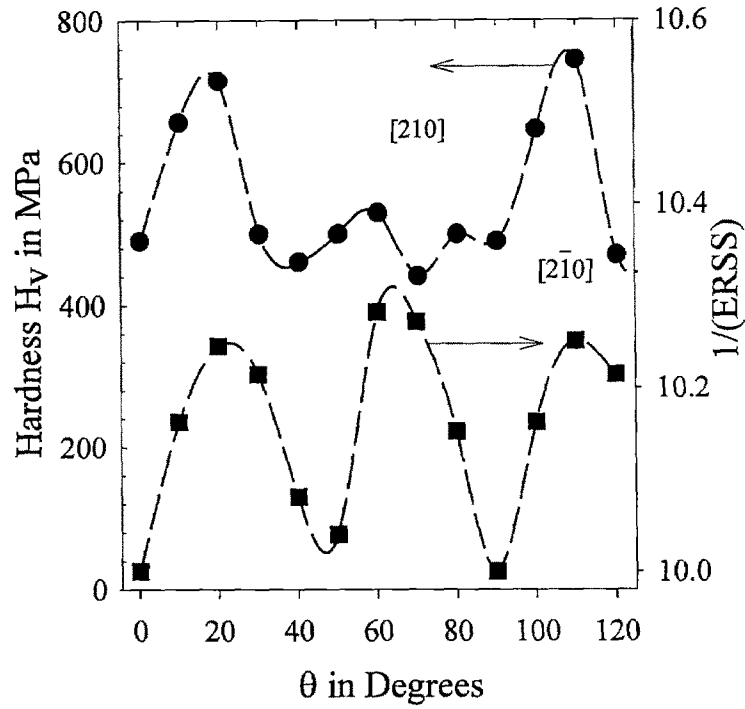


Fig. 3.7. Plots of Hardness, H_v , of the (001) plane and the reciprocal of the effective resolved shear stress versus azimuthal orientation of the indenter.

3.5.Creep

Since the mobility of atoms increases rapidly with temperature, it can be appreciated that diffusion-controlled processes can have a very significant effect on high temperature mechanical properties. High temperature will also result in greater mobility of dislocations by the mechanisms of climb. The equilibrium concentration of vacancies likewise increases with temperature. New deformation mechanisms may come into play at elevated temperatures. However, at elevated temperature the strength becomes very dependent on both strain rate and time of exposure.

The time-dependent plastic deformation of materials subjected to a constant load (or stress) and temperatures greater than about $0.4T_m$ is termed creep, where T_m is the melting point on absolute scale. A typical creep curve (strain versus time) will normally exhibit three distinct regions. For transient (or primary) creep, this rate (or slope) diminishes with time. The plot becomes linear (i.e., creep rate becomes constant) in the steady-state (or secondary) region. And finally, deformation accelerates for tertiary creep, just prior to failure (or rupture).

Both temperature and the level of the applied stress influence the creep characteristics. At a temperature substantially below $0.4T_m$, and after the initial deformation, the strain is virtually independent of time. With either increasing stress or temperature, the following effects are noted:

1. the instantaneous strain at the time of stress application increases
2. the steady-state creep rate is increased; and
3. the rupture lifetime is diminished.

Analytical expressions relating creep rate to both temperature and stress are presented in literature of mechanical metallurgy. Several theoretical mechanisms have been proposed to explain the creep behaviour for various materials; these mechanisms involve stress-induced vacancy diffusion, grain boundary diffusion, dislocation diffusion, and grain boundary sliding. Creep mechanisms may be discerned on the basis of steady-state rate stress exponent and creep activation energy values. In addition, correlation has been made between the activation energy for creep and activation energy for diffusion.

3.5.1. Effect of temperature and loading time on the microhardness of Zinc

(tris) Thiourea Sulphate crystal

For this study, the hardness indentations were produced on the as-grown (100) face of the crystal. For the higher temperature testing, a simple hot stage giving temperatures up to 100⁰ C was used with the hardness tester. The temperature was monitored using a copper-constantan thermocouple. The thermocouple leads were connected to the input terminals of an operational voltage amplifier of gain 100 and the output was read to an accuracy of 1 mV. Before producing the indentations, the specimen to be indented was held at the desired temperature for at least 30 minutes to achieve thermal equilibrium.

In our study of indentation under different applied loads, there was no fracture observed under applied loads up to at least 250 gm. Hence for the loading time dependence study, a constant load of 20 gm was maintained. Also no fracture was observed under optical microscope up to the maximum loading time (viz., 120 sec) used in the experiments. The most important characteristic of time dependent strain is its

sensitivity to temperature, which increases with temperature. The deformation rate under given conditions of temperature and stress may depend on such factors as density and arrangement of dislocations, vacancies, their interactions and the type of impurities present in the crystal. These factors themselves depend in a complex manner on the mechanical and thermal history of the crystal. The loading time dependence of the hardness at different temperatures as obtained on the as-grown (100) face is shown in the plots of figure 3.8, the hardness decreases with increasing loading time. The hardness behaviour in this respect is known to closely parallel the creep characteristics obtained in unidirectional stress tests. The general behaviour may be described by an overall empirical relation.^{16, 17} In the present study, the relation based on the kinematic analysis of the creep process during indentation has been found to be applicable and it has been used to evaluate the activation energy for creep.

$$\ln(H_v^{-3} - H_0^{-3}) = \ln A + \ln(t^{1/3} - t_0^{1/3}) - \frac{Q}{3RT} \quad (A)$$

The plots of $\ln H_v$ against $\ln t$ were obtained at different temperatures as shown in figure 3.9.

It can be seen that $\ln H_v$ varies linearly with $\ln t$ and the slope of the straight lines increases with temperature as predicted by Atkins *et al*¹⁸. For each temperature, H_{v0} is obtained for $t_0 = 1$ second from these plots. Figure 3.10 shows the plots of $\ln (H_v^{-3} - H_{v0}^{-3})$ versus $\ln (t^{1/3} - t_0^{1/3})$ at four different temperatures, namely, 295° K, 323° K, 338° K and 348° K. These are straight lines, all of almost equal slopes, close to unity in accordance with the above equation. The plots yield the average creep activation energy, $Q = 36.6$ Kcal/mole. Of the factors known to affect the deformation creep, dislocation motion is the most dominant one. Therefore the energy barriers that the dislocations have to overcome and the role of thermal energy in overcoming such barriers determine the creep activation. However, the thermal energy can activate deformation mechanisms involving only a relatively small number of atoms rather than long dislocation segments. In the present case, where the crystal is non-metallic, the dislocation mobility is expected to be small and hence the progress of strain with time may only be effected by thermal diffusion or by mechanisms like dislocation climb which involves only addition or removal of a single atom at a time on an edge jog.¹⁶ Nevertheless, since the temperatures involved are above $0.5T/T_m$ where $T_m =$ absolute melting point, the creep activation may be supported by self-diffusion as found in metals at such temperatures (Atkins *et al.*, Bhatt *et al*).^{18, 19}

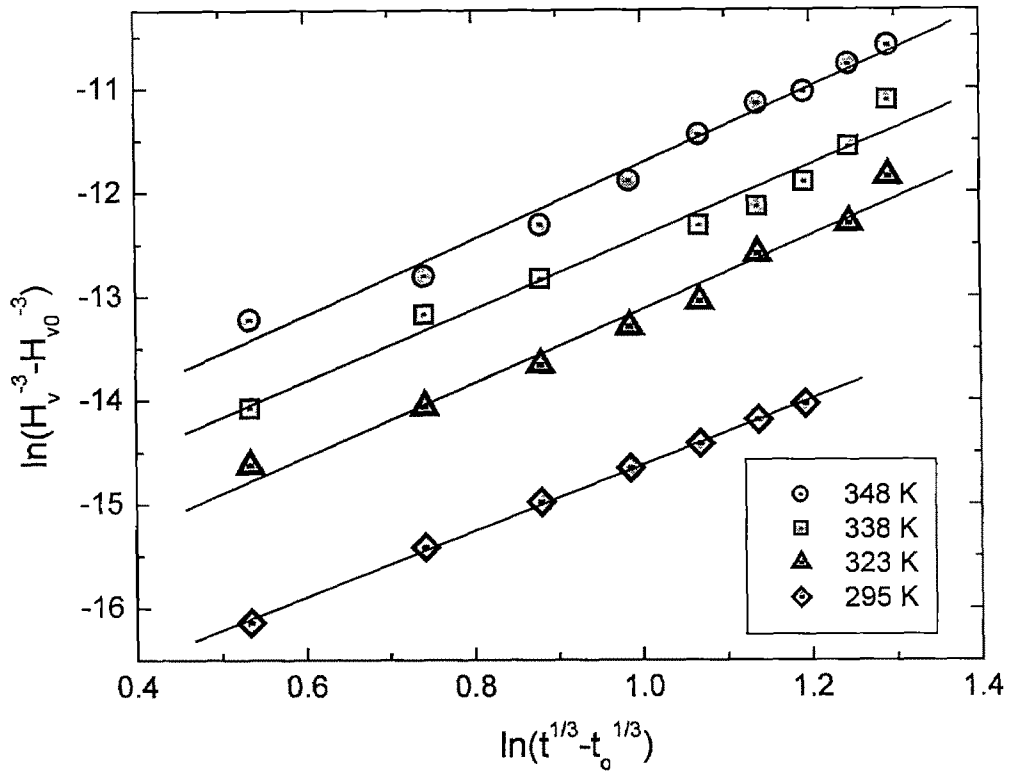


Fig. 3.10. The figure shows the plots of $\ln(H_v^{-3} - H_{v0}^{-3})$ versus $\ln(t^{1/3} - t_0^{1/3})$ at four different temperatures, viz., 295 K, 323 K, 338 K and 348 K.

3.6. Conclusions:

The hardness versus load studies indicate that at low loads, the hardness increases with increasing load and exhibits a peak before reaching saturation at higher loads. It is observed that (100) is the hardest of the three planes under study. The surface anisotropy coefficients of the Vickers hardness of (100), (010) and (001) planes have been found to be 0.35, 0.49 and 0.42, respectively. The hardest and the softest directions on the three planes were analysed stereographically. The Vickers hardnesses of (100) and (001) planes exhibit significant surface anisotropy following the anisotropy in resolved shear stress on the active slip system of the crystal. The indentation time dependence of the Vickers hardness of the as-grown (100) face of the ZTS crystal has been found to strongly depend on the temperature. The indentation creep observed agrees with the kinematic model proposed by Atkins et al and accordingly, the activation energy for creep has been found to be 36.5 Kcal/mole.

REFERENCES

1. Gilman in "*The Science of Hardness testing and Its Research Applications*", (eds.) J. H. Westbrook and H Conrad, (ASM, Ohio), (1973).
2. "*Hardness Testing*", edited by H. E. Boyer, ASM INTERNATIONAL (1987).
3. E. B. Bergsman, ASTM Bull. **176**, pp. 37-43, September, (1951).
4. H. Buckle, Metall.Rev. Vol.4, No.3 pp.49-100,(1959).
5. Smith, R. L., and Sandland, G. E., "*Some Notes on the Use of a Diamond Pyramid for Hardness Testing,*" J. Iron Steel Inst. (London), III (1925).
6. G. R. Pandya, D. D. Vyas and C. F. Desai, Cryst. Res.& Tech. **22**, 381 (1984).
7. V. P. Bhatt, R. M. Patel and C. F. Desai, Cryst. Res. & Tech. **18**,9,1173 (1983).
8. Brookes, C. A. and Moxley, B, J. Phys. E **8**, 456, (1975)).
9. Rowcliffe, D. J. and Hollox, G. O., Vrown Boveru Res. Reports KLR **71**, 14 (1971).
10. Hannlink, R. H. J. *et al*, Phy. Status Solidi A **6**, K26 (1971).
11. F. W. Daniels and C. G. Dunn, Trans ASM, **41**, 419 (1949)
12. Brookes, C. A., O'Neill, J. B. and Redfern, A. W. Proc. Roy. Soc. A **73**,322 (1971).
13. C. S. Barret and Massalski, "*Structure of Metals*", 3rd edition, p.30. Mc Graw-Hill, New York, (1966).
14. V. Venkataramanan, G. Dhanaraj, V.K. Wadhawan, J.N. Sherwood and H. L. Bhat, J Cryst. Growth **92**, 154 (1995).
15. Bhatt, V. P., Desai, C. F., Shah, R. C.: Res Mechanica **9**, 35-40 (1983).
16. Ito K, Sci. Pap. Sendai tohoku, Uni. Ser 1 **12** 137 (1923).
17. Shishokin V. P., Z. Anorg. Chem **189**, 263 (1930).

18 Atkins A G, Silverio A and Tabor D J. *Inst. Met.* **94** 369 (1966).

19 Bhatt, V. P. and Desai C. F; *Bull mater. Sci.* **4**, 23 (1982)